Int. J. Electrochem. Sci., 16 **(2021)** Article ID: 210439, doi: 10.20964/2021.04.13

International Journal of
ELECTROCHEMICAL
SCIENCE
www.electrochemsci.org

Mini review

Energy Storage Device Application Based on MXenes Composites: a Mini Review

Jun Lv[*]*, Qinghua Huang, Tiejun Liu and Qiaoyu Pan*

School of Intelligent Manufacturing, Zhejiang Guangsha Vocational and Technical University of Construction, No. 1 Guangfu East Road, Dongyang City, Zhejiang Province, 322100, P.R. China
[*]E-mail: junlv@vtcuni.com

Received: 8 December 2020 / *Accepted:* 15 January 2021 / *Published:* 28 February 2021

With the rapid development of wearable electronic products, increasing attention has been given to flexible energy storage devices. MXenes are a kind of two-dimensional graphene material discovered in recent years. This material has ultra-high volume specific capacity, metal-level conductivity, good hydrophilicity and rich surface chemistry, so it has been widely used in flexible energy storage electrode materials. MXene materials also have some shortcomings that need to be solved, such as easy oxidation and dense interlayer stacking in a water/oxygen environment. At present, there is no comprehensive introduction to the research progress, advantages and disadvantages of MXenes in the field of flexible energy storage devices. Therefore, this review outlines the research progress of MXene-based nanocomposites (MXenes, MXenes/carbon, MXenes/metal oxide, MXenes/polymer) in the field of flexible energy storage electronic devices. This review summarizes the research progress of MXenes from three aspects: flexible capacitors, flexible batteries and flexible sensors. We compared MXenes with other two-dimensional materials in terms of synthesis methods and physical properties (such as conductivity and stress-strain properties), and discussed the problems and challenges faced by MXenes in the practical application of flexible devices. We also objectively discuss the development direction of MXenes in flexible energy storage devices.

Keywords: MXenes; Energy storage device; Two-dimensional material; Two-dimensional materials; Nanocomposite

1. INTRODUCTION

With the increasing demand for wearable electronic products, flexible energy storage devices have been rapidly developed. MXenes are considered to be promising flexible electrodes because of their ultra-high volume specific capacity, metal conductivity, excellent hydrophilicity and abundant surface chemical properties [1–5]. MXenes and MXene-based composites are widely used in flexible electronic devices such as sensors, nanogenerators and electromagnetic interference shielding [6–9]. In

addition, the stress, strain, conductivity, capacitance and other properties affected by the application of MXenes in flexible devices have been used to maintain the balance of mechanical and electrochemical properties in the design of flexible devices [10–15].

Different from the carbon-based materials, flexible supercapacitors (SCs) are expected to have high energy density. First, MXene materials exhibit ultra-high bulk energy density due to their high energy density and large Faraday pseudocapacitance (derived from their rich surface chemistry) [16–25]. Furthermore, MXenes can also be used as collectors because of the electrical conductivity of the metal. Therefore, a flexible electrode is expected to be completely built on a flat MXene layer to improve the bulk energy density of flexible SCs and provide power for wear-resistant electrons [18,19,26–30]. For flexible MXene matrix composites, carbon materials have been used, such as reduced graphene oxide (RGO) and carbon nanotubes (CNTs). This strategy effectively prevents the restacking of MXene sheets and significantly improves flexibility. Polymers are another promising additive that could be used together with MXenes to greatly enhance the mechanical properties of materials [31–34]. MXenes can optimize mechanical strength without sacrificing conductivity [35–38]. In addition, metal oxides with high Faraday pseudocapacitance can also be used to bond with MXenes to obtain high electrochemical performance. These nanocomposite methods are helpful to prepare flexible MXene-based SCs [39–42]. These materials have excellent flexibility, high specific capacity and good mechanical performance to provide power for wearable electronic products. Although the above flexibility and mechanical strength have been improved, the use of the substrate not only complicates the manufacturing process but also reduces the stability of the structure due to the loose connection between the electrode material and the substrate [43–45].

Currently, intelligent wearable electronic products with increasingly complex functions require energy storage devices with a high energy density and minimum volume, which makes energy batteries more competitive than power supercapacitors [46–50]. MXene materials have metal conductivity, volume specific capacity and rich surface chemistry, which are expected to solve some application problems [51–55]. In addition, MXenes-unbonded film electrodes can be used for maintaining a high-volume specific capacity. For example, Du and co-workers reported a Ti_3C_2Tx-MXene whose surface is modified by pyrite nanodots [56]. This composite material has excellent rate performance when used for lithium-/sodium-ion storage, especially for lithium-ion storage. After 1000 cycles, at 10 A/g, a reversible specific capacity of 762 mAh/g can be obtained. For the storage of sodium ions, the FeS_2@MXene nano-hybrid also provides a reversible specific capacity of 563 mAh/g. After 100 cycles, the current density is 0.1 A/g.

2. FLEXIBLE MXENE-BASED MATERIAL

2.1. MXenes/carbon-based composite

Figure 1 shows the $Ti_3C_2T_x$/graphene/PDMS layered structure. It contains two layers after stretching: a brittle upper layer dominated by $Ti_3C_2T_x$ and a flexible graphene/PDMS composite bottom layer. The coordinated movement of the upper and lower layers breaks and maintains the balance between the conductive paths, ensuring that the sensor has a high and stable gauge coefficient in a wide

strain range (for example, the strain range is 0–52.6% and 52.6–74.1% when the strain coefficients are 190.8 and 1148.2, respectively). The strain sensor based on the $Ti_3C_2T_x$/graphene/PDMS-layered structure also has a low detection limit with high linearity, high cycle stability (more than 5000 cycles) and resistance to all-round human motion monitoring. Pan and Ji used nitrogen- and oxygen-co-doped C and Ti_3C_2 for compounding [57–61]. The concentration of nitrogen and oxygen doping will change with the change in the reaction atmosphere, thereby affecting the electrochemical performance of the electrode material. The excellent electrical properties give the composite material a specific capacitance of 250.6 F/g at 1A/g. The retention rate after 5000 cycles is 94%. In addition, N and O co-doped C@Ti_3C_2 composite symmetrical supercapacitors have an energy density of 10.8 Wh/kg when the power density is 600 W/kg.

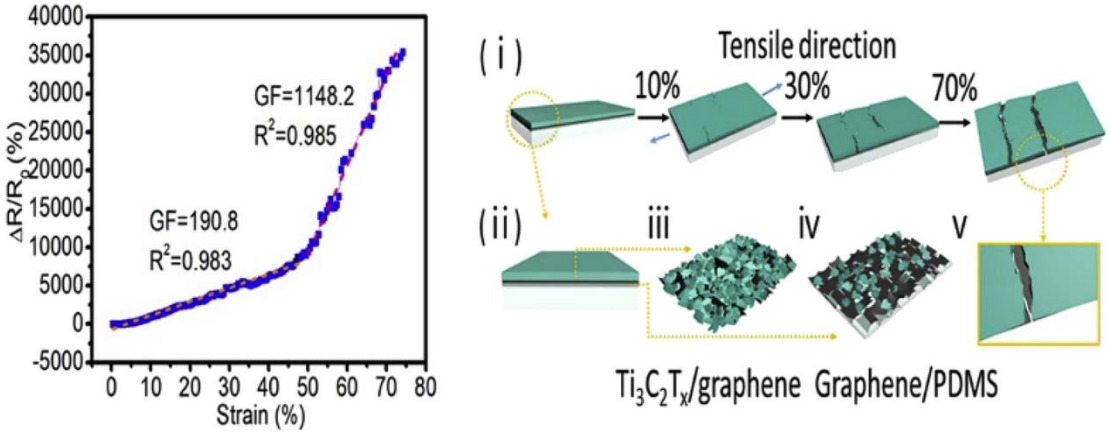

Figure 1. Layered structure of the $Ti_3C_2T_x$/graphene/PDMS composite and its performance. Reprinted with permission from reference [62]. Copyright 2019 Elsevier.

Li et al reported the uniform electrodeposition of Ni Al LDH on MXenes [62]. MXene was then deposited by low-pressure chemical vapor deposition (CVD) in argon at 700 °C. The MWCNTs are used not only as a spacer to prevent the re-clogging of the MXene film but also as a charge collector within and between the layers. In addition, the three-dimensional interconnection structure effectively improves the mechanical and physicochemical stability of the composite electrode. The voltage window of MXenes is narrow. This shortcoming prevents it from being made into a supercapacitor with high energy density. Hu et al. [63] proposed a positive electrode using a $Ti_3C_2T_x$-MXene cathode and redox-active hydroquinone/carbon nanotubes. The two electrodes are separated by a Nafion membrane. During charging and discharging, hydrogen ions shuttle back and forth between the cathode and anode. This process can be used for charge compensation while improving the electrochemical performance of the device.

2.2. Mxene/MnO_2 composite material

Compared with carbon nanomaterials, transition metal oxides such as MnO_2 have ultra-high pseudocapacitance, which is beneficial for significantly improving the low energy density of SCs [64–67]. Therefore, it is best to combine transition metal oxides with MXenes to further increase the volumetric capacitance. The hybrid membrane electrode used in SCs.

Zhou et al. [68] recently proposed a composite material of MnO_2 and MXene on carbon fibre cloth. Due to the synergistic effect, the new electrode has excellent electrochemical performance (511.2 After 10,000 cycles, the capacitance of the composite electrode decreased by only 17%. Figure 2 shows a schematic diagram of MnO_2 nanorod/MXene/carbon cloth synthesis. In an article published in 2017, a simple and scalable hybrid filtration method was used to develop a MnO_2/Ti_3C_2 hybrid material with a molecular stacking structure [69]. The advantages of these materials have been combined in a composite material, thereby providing excellent electrochemical performance. The highly flexible and symmetrical supercapacitor based on the new hybrid electrode has first-class electrochemical performance. The maximum energy and power density are 8.3 Wh/kg (221.33 W/kg) and 2376 W/kg (at 3.3 Wh/kg). This supercapacitor has good energy density and power density regardless of the bending state. This shows the great possibility of application in future flexible and portable micro-power systems.

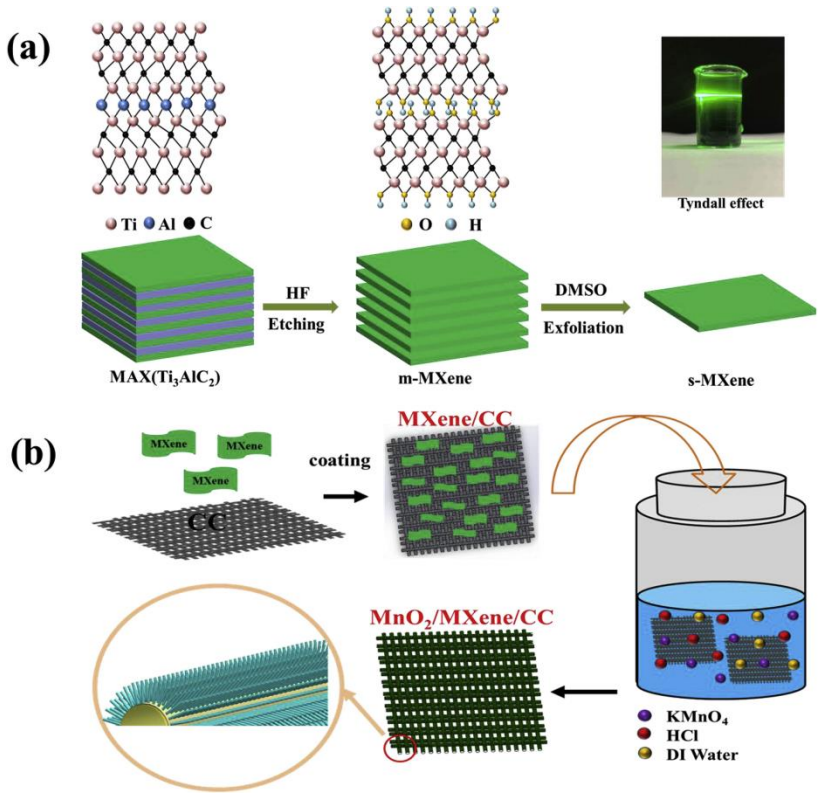

Figure 2. (a) Schematic diagram of s-MXene Synthesis. (b) Schematic diagram of MnO_2/MXene/CC composite preparation. Reprinted with permission from reference [68] Copyright 2020 Elsevier.

2.3. MXene-polymer composite

Mechanical properties such as the strength and flexibility of flexible SCs in wear-resistant electronic products are as important as electrochemical properties [70–72]. The insertion of polymers between MXene layers can enhance molecular-level coupling. This close combination can effectively enhance the strength and flexibility of the hybrid film and effectively reduce the oxidation of MXene. Polyvinyl shows great potential in the preparation of MXene-based thin-film electrodes due to its high solubility in water and abundant hydroxyl groups on the molecular chain. This type of electrode has abundant negative oxygen and fluorine groups, which can be used to form hydrogen bonds between polyvinyl alcohol and MXene. For example, Lin et al [73] created a flexible conductive material, MXene@polyvinyl alcohol, through a vacuum-assisted filtration film. This film maintains high electronic conductivity while achieving a perfect match between mechanical and electrochemical properties. This film is expected to meet the rigidity requirements of flexible SCs to power consumer electronics. Similarly, Sobolčiak et al. [74] successfully prepared $Ti_3C_2T_x$-polyvinyl nanofibres using electrospinning technology. The layered $Ti_3C_2T_x$ nanosheet has a hydrophilic surface and good electrical conductivity, making it an ideal filler for high-performance nanocomposites. Dynamic mechanical analysis showed that the elastic modulus of the composite material increased from 392 MPa to 855 MPa. In addition, the direct current conductivity of $Ti_3C_2T_x$-polyvinyl nanofibres is 0.8 ms/cm. The mechanical and electrical properties of the $Ti_3C_2T_x$-polyvinyl composite make it a viable material for high-performance energy applications.

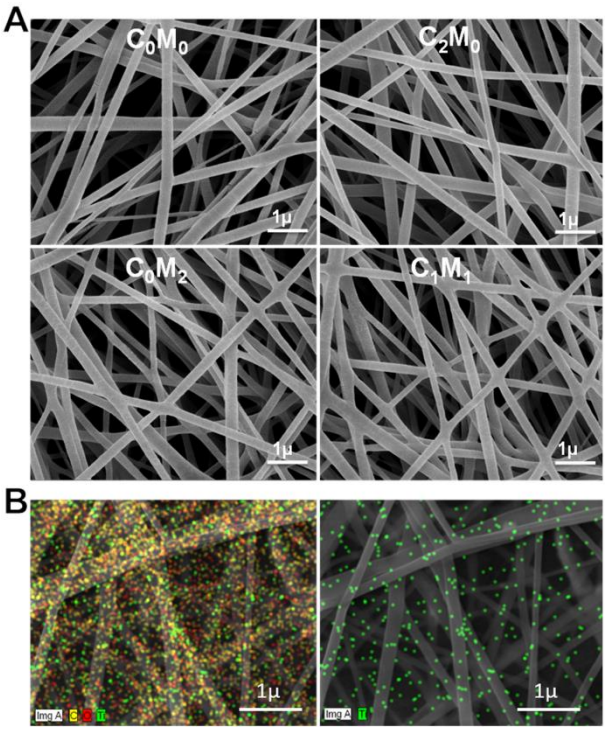

Figure 3. (A) SEM images of the reinforced polyvinyl nanofibres at different loadings of $Ti_3C_2T_x$. (B) EDS mapping. Reprinted with permission from reference [74] Copyright 2020 Plos One.

3. MXENES-BASED FLEXIBLE DEVICE

Two-dimensional MXenes combine many characteristics, such as layered structures, rich surface chemistry, metal conductivity and hydrophilicity. MXenes have advantages over other widely studied 2D materials (graphene, MoS_2, etc.). Wang et al. [75] used HF to etch Al in Ti_3AlC_2, prepared a Ti_3C_2 nanomaterial for immobilizing haemoglobin, and prepared a dielectric-free biosensor. Spectroscopy and electrochemical results confirmed that Ti_3C_2 has a good immobilization ability and biocompatibility for haemoglobin. Due to the special structure and properties of Ti_3C_2, it is conducive to the direct electron transfer of haemoglobin. Therefore, this sensor has good detection performance for H_2O_2.

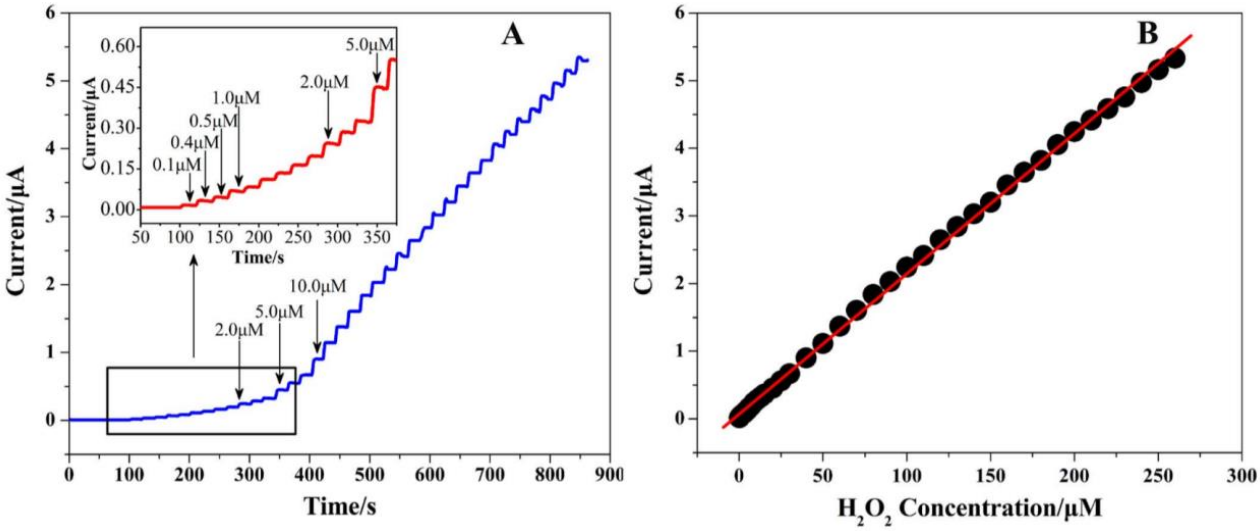

Figure 4. (A) Typical I-T curve of the Ti_3C_2-based sensor at -0.35 V to successive addition of H_2O_2. (B) The steady-state current vs. H_2O_2 concentration. Reprinted with permission from reference [75] Copyright 2020 IOP.

The flexible $Ti_3C_2T_x$/GO electrode made by inkjet printing technology has excellent H_2O_2 detection performance. In addition, MXenes were found to be able to sense bromate (BrO_3) and volatile organic compound (VOC) gases, such as NH_3 and CH_3COCH_3 [76]. Wan et al. [77] reported a flexible wearable transient stress sensor with MXene sheets, which can be used for high sensitivity, reproducibility, wireless, degradability and wide-range (up to 30 kPa) human-computer interfaces. A flexible stress sensor was fabricated by impregnating MXene into tissue paper and sandwiching it between a biodegradable PLA sheet and a PLA sheet with a cross finger conducting electrode. Stress sensors are connected to human skin to obtain a wide range of biological monitoring data from small deformation to large movement.

Under the action of an external force, the interlayer spacing in MXene and the spacing between MXene particles will produce corresponding compression, which makes the conductivity of the sensitive layer of the MXene material change, and the resistance value changes accordingly [78]. To further improve the deformation space of MXene under pressure, scientists use the confinement effect of the

micro-channel structure to make the distribution of MXene in the device form a three-dimensional stacked structure. The sensor can detect human pulses, throat micro-motions, object accelerations and even sound signals, which shows the incredibly high sensitivity of the sensor. This single-structure design idea can effectively reduce the volume proportion of sensor elements in electronic devices while achieving multifunctional detection, which provides a new idea for the development of future sensors. Yue et al. [79] reported a dipping process to prepare an MXene sponge and apply it to a piezoresistive sensor using polyvinyl alcohol nanowires as a spacer layer. The detection limit of this sensor can reach 9 Pa, and the fast response time is as low as 138 ms. This new type of MXene sponge sensor can realize real-time monitoring of human physiological signals. Figure 5 shows the MXene sponge preparation and sensor fabrication process.

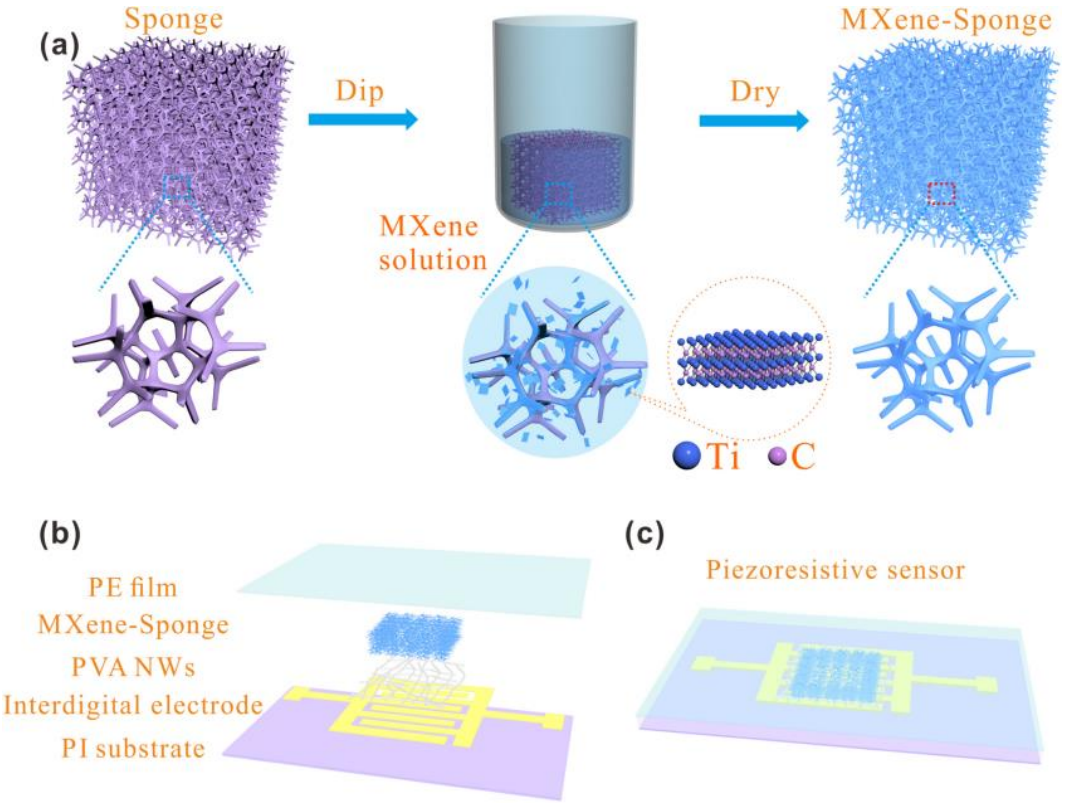

Figure 5. (a) Scheme of preparation of MXene-sponge. (b, c) Scheme of sensor preparation. Reprinted with permission from reference [79] Copyright 2020 Elsevier.

The electrochemical performance of M_2CH_2(M = Ti or V) MXene as a cathode material for FIBs has been studied [80]. First, the structural stability of M_2CH_2 is calculated using first-principle calculations. Second, the favourable adsorption site is determined by analysing the adsorption energy. The electronic performance and charge compensation mechanism are studied. In addition, by calculating the migration energy barrier on the possible micro-diffusion path, the F-mobility of the surface of the M_2CH_2 monolayer can be predicted. In particular, the biaxial strain loading scheme (tension/compression) is used to comprehensively explore the F migration energy barrier under various strain states. It is important to study the voltage distribution by gradually introducing F on the surface of

the M_2CH_2 monolayer to simulate the F-embedding/de-embedding process and evaluate the corresponding specific energy.

4. CONCLUSIONS AND OUTLOOKS

Flexible energy storage devices represent a rapidly developing research direction and show great potential. In the context of minimizing wearable electronic devices, the investigation of MXenes have been carried out due to the insurmountable volume ratio capacitance in recent years. The important problems faced by two-dimensional nanomaterials force researchers to turn to freeze-drying or sandwich structures. At the same time, compared with pure MXenes with low transverse size, the construction of sandwich structures using polymers can improve the mechanical property. Due to the importance of mechanical strength and flexibility, carbon nanomaterials are mainly used in combination with MXenes through vacuum filtration. Inspired by these hybrid strategies, the high pseudo-capacitance of transition metal oxides combined with MXenes can significantly improve the specific capacitance.

To date, although some achievements have been made in the application of MXene-based composites, there are still some challenges. One of the problems facing scientists is the non-negligible ion diffusion resistance in the vertical direction, which greatly reduces the rate ability at high current density. The application of MXenes in water-based flexible batteries need to solve the oxidation problem. Advanced deposition techniques in an inert atmosphere at room temperature are considered to be a possible way to solve the oxidation problem and improve the chemical stability of aqueous electrolytes. Furthermore, loading MXenes without using binders is the key point in the future work.

References

1. X. Tang, X. Guo, W. Wu, G. Wang, *Adv. Energy Mater.*, 8 (2018) 1801897.
2. Y. Wu, P. Nie, L. Wu, H. Dou, X. Zhang, *Chem. Eng. J.*, 334 (2018) 932–938.
3. J. Zhu, R. Shi, Y. Liu, Y. Zhu, J. Zhang, X. Hu, L. Li, *Appl. Surf. Sci.*, 528 (2020) 146985.
4. H. Kaland, J. Hadler-Jacobsen, F.H. Fagerli, N.P. Wagner, Z. Wang, S.M. Selbach, F. Vullum-Bruer, K. Wiik, S.K. Schnell, *Sustain. Energy Fuels*, 4 (2020) 2956–2966.
5. H. Liu, H. Wang, Z. Jing, K. Wu, Y. Cheng, B. Xiao, *J. Phys. Chem. C*, 124 (2020) 25769–25774.
6. Z. Wang, N. Zhang, M. Yu, J. Liu, S. Wang, J. Qiu, *J. Energy Chem.*, 37 (2019) 183–191.
7. D.K. Lee, Y. Chae, H. Yun, C.W. Ahn, J.W. Lee, *ACS Nano*, 14 (2020) 9744–9754.
8. H. Shi, C.J. Zhang, P. Lu, Y. Dong, P. Wen, Z.-S. Wu, *ACS Nano*, 13 (2019) 14308–14318.
9. C. Du, J. Wu, P. Yang, S. Li, J. Xu, K. Song, *Electrochimica Acta*, 295 (2019) 1067–1074.
10. H. Tang, W. Li, L. Pan, C.P. Cullen, Y. Liu, A. Pakdel, D. Long, J. Yang, N. McEvoy, G.S. Duesberg, V. Nicolosi, C. (John) Zhang, *Adv. Sci.*, 5 (2018) 1800502.
11. Z. Shamsadin-Azad, M.A. Taher, S. Cheraghi, H. Karimi-Maleh, *J. Food Meas. Charact.*, 13 (2019) 1781–1787.
12. H. Karimi-Maleh, F. Karimi, Y. Orooji, G. Mansouri, A. Razmjou, A. Aygun, F. Sen, *Sci. Rep.*, 10 (2020) 11699.

13. H. Karimi-Maleh, F. Karimi, S. Malekmohammadi, N. Zakariae, R. Esmaeili, S. Rostamnia, M.L. Yola, N. Atar, S. Movaghgharnezhad, S. Rajendran, A. Razmjou, Y. Orooji, S. Agarwal, V.K. Gupta, *J. Mol. Liq.*, 310 (2020) 113185.
14. L. Fu, Z. Liu, J. Ge, M. Guo, H. Zhang, F. Chen, W. Su, A. Yu, *J. Electroanal. Chem.*, 841 (2019) 142–147.
15. J. Zhou, Y. Zheng, J. Zhang, H. Karimi-Maleh, Y. Xu, Q. Zhou, L. Fu, W. Wu, *Anal. Lett.*, 53 (2020) 2517–2528.
16. F. Ming, H. Liang, W. Zhang, J. Ming, Y. Lei, A.-H. Emwas, H.N. Alshareef, *Nano Energy*, 62 (2019) 853–860.
17. F. Liu, Y. Liu, X. Zhao, X. Liu, L.-Z. Fan, *J. Mater. Chem. A*, 7 (2019) 16712–16719.
18. Y. Zhang, Z. Mu, C. Yang, Z. Xu, S. Zhang, X. Zhang, Y. Li, J. Lai, Z. Sun, Y. Yang, Y. Chao, C. Li, X. Ge, W. Yang, S. Guo, *Adv. Funct. Mater.*, 28 (2018) 1707578.
19. Y. Li, D. Xu, D. Zhang, Y. Wei, R. Zhang, Y. Guo, *RSC Adv.*, 9 (2019) 33572–33577.
20. K. Fan, Y. Ying, X. Li, X. Luo, H. Huang, *J. Phys. Chem. C*, 123 (2019) 18207–18214.
21. Q. Meng, J. Ma, Y. Zhang, Z. Li, A. Hu, J.-J. Kai, J. Fan, *J. Mater. Chem. A*, 6 (2018) 13652–13660.
22. Q. Huang, J. Lv, R. Mei, Z. Tian, L. Li, *Fluid Transm. Control*, 11 (2016) 17–24.
23. Q. Pan, J. Lv, Q. Huang, G. Mei, *Mech. Eng. Mater.*, 5 (2019) 87–93.
24. T. Liu, L. Qing, Q. Pan, B. Wang, *Rubber Plast. Technol. Equip.*, 4 (2016) 55–63.
25. T. Liu, Q. Pan, M. Zhang, W. Shi, *Met. Process.*, 5 (2017) 5–15.
26. L. Fu, Y. Zheng, P. Zhang, H. Zhang, Y. Xu, J. Zhou, H. Zhang, H. Karimi-Maleh, G. Lai, S. Zhao, W. Su, J. Yu, C.-T. Lin, *Biosens. Bioelectron.*, 159 (2020) 112212.
27. X. Zhang, R. Yang, Z. Li, M. Zhang, Q. Wang, Y. Xu, L. Fu, J. Du, Y. Zheng, J. Zhu, *Rev. Mex. Ing. Quím.*, 19 (2020) 281–291.
28. L. Fu, A. Wang, K. Xie, J. Zhu, F. Chen, H. Wang, H. Zhang, W. Su, Z. Wang, C. Zhou, S. Ruan, *Sens. Actuators B Chem.*, 304 (2020) 127390.
29. H. Karimi-Maleh, F. Karimi, M. Alizadeh, A.L. Sanati, *Chem. Rec.*, 20 (2020) 682–692.
30. H. Karimi-Maleh, Y. Orooji, A. Ayati, S. Qanbari, B. Tanhaei, F. Karimi, M. Alizadeh, J. Rouhi, L. Fu, M. Sillanpää, *J. Mol. Liq.* (2020) 115062.
31. Z. Li, X. Wang, W. Zhang, S. Yang, *Chem. Eng. J.*, 398 (2020) 125679.
32. Z. Xiao, Z. Li, P. Li, X. Meng, R. Wang, *ACS Nano*, 13 (2019) 3608–3617.
33. S.-Y. Pang, Y.-T. Wong, S. Yuan, Y. Liu, M.-K. Tsang, Z. Yang, H. Huang, W.-T. Wong, J. Hao, *J. Am. Chem. Soc.*, 141 (2019) 9610–9616.
34. R. Venkatkarthick, N. Rodthongkum, X. Zhang, S. Wang, P. Pattananuwat, Y. Zhao, R. Liu, J. Qin, *ACS Appl. Energy Mater.*, 3 (2020) 4677–4689.
35. M. Xu, S. Lei, J. Qi, Q. Dou, L. Liu, Y. Lu, Q. Huang, S. Shi, X. Yan, *ACS Nano*, 12 (2018) 3733–3740.
36. J. Song, X. Guo, J. Zhang, Y. Chen, C. Zhang, L. Luo, F. Wang, G. Wang, *J. Mater. Chem. A*, 7 (2019) 6507–6513.
37. Y. Dong, H. Shi, Z.-S. Wu, *Adv. Funct. Mater.*, 30 (2020) 2000706.
38. X. Zhang, L. Wang, W. Liu, C. Li, K. Wang, Y. Ma, *ACS Omega*, 5 (2020) 75–82.
39. Q. Zhao, Q. Zhu, J. Miao, P. Zhang, B. Xu, *Nanoscale*, 11 (2019) 8442–8448.
40. H. Shi, M. Yue, C.J. Zhang, Y. Dong, P. Lu, S. Zheng, H. Huang, J. Chen, P. Wen, Z. Xu, Q. Zheng, X. Li, Y. Yu, Z.-S. Wu, *ACS Nano*, 14 (2020) 8678–8688.
41. M. Shang, X. Chen, B. Li, J. Niu, *ACS Nano*, 14 (2020) 3678–3686.
42. C. Xiong, G.Y. Zhu, H.R. Jiang, Q. Chen, T.S. Zhao, *Energy Storage Mater.*, 33 (2020) 147–157.
43. H. Karimi-Maleh, O.A. Arotiba, *J. Colloid Interface Sci.*, 560 (2020) 208–212.
44. H. Karimi-Maleh, B.G. Kumar, S. Rajendran, J. Qin, S. Vadivel, D. Durgalakshmi, F. Gracia, M. Soto-Moscoso, Y. Orooji, F. Karimi, *J. Mol. Liq.*, 314 (2020) 113588.

45. L. Fu, K. Xie, D. Wu, A. Wang, H. Zhang, Z. Ji, *Mater. Chem. Phys.*, 242 (2020) 122462.
46. S. Sun, Z. Xie, Y. Yan, S. Wu, *Chem. Eng. J.*, 366 (2019) 460–467.
47. G. Jiang, N. Zheng, X. Chen, G. Ding, Y. Li, F. Sun, Y. Li, *Chem. Eng. J.*, 373 (2019) 1309–1318.
48. B. Liu, L. Yu, F. Yu, J. Ma, *Desalination* (2020) 114897.
49. F. Zhang, X. Guo, P. Xiong, J. Zhang, J. Song, K. Yan, X. Gao, H. Liu, G. Wang, *Adv. Energy Mater.*, 10 (2020) 2000446.
50. B. Chen, A. Feng, R. Deng, K. Liu, Y. Yu, L. Song, *ACS Appl. Mater. Interfaces*, 12 (2020) 13750–13758.
51. X. Guo, J. Zhang, J. Song, W. Wu, H. Liu, G. Wang, *Energy Storage Mater.*, 14 (2018) 306–313.
52. P. Ridley, C. Gallano, R. Andris, C.E. Shuck, Y. Gogotsi, E. Pomerantseva, *ACS Appl. Energy Mater.*, 3 (2020) 10892–10901.
53. Y. Fang, R. Hu, B. Liu, Y. Zhang, K. Zhu, J. Yan, K. Ye, K. Cheng, G. Wang, D. Cao, *J. Mater. Chem. A*, 7 (2019) 5363–5372.
54. Z. Xiao, Z. Li, X. Meng, R. Wang, *J. Mater. Chem. A*, 7 (2019) 22730–22743.
55. M.K. Aslam, Y. Niu, M. Xu, *Adv. Energy Mater.*, n/a (2020) 2000681.
56. C.-F. Du, Q. Liang, Y. Zheng, Y. Luo, H. Mao, Q. Yan, *ACS Appl. Mater. Interfaces*, 10 (2018) 33779–33784.
57. Z. Pan, X. Ji, *J. Power Sources*, 439 (2019) 227068.
58. L. Fu, Q. Wang, M. Zhang, Y. Zheng, M. Wu, Z. Lan, J. Pu, H. Zhang, F. Chen, W. Su, *Front. Chem.*, 8 (2020) 92.
59. Y. Xu, Y. Lu, P. Zhang, Y. Wang, Y. Zheng, L. Fu, H. Zhang, C.-T. Lin, A. Yu, *Bioelectrochemistry*, 133 (2020) 107455.
60. M. Zhang, B. Pan, Y. Wang, X. Du, L. Fu, Y. Zheng, F. Chen, W. Wu, Q. Zhou, S. Ding, *ChemistrySelect*, 5 (2020) 5035–5040.
61. J. Ying, Y. Zheng, H. Zhang, L. Fu, *Rev. Mex. Ing. Quím.*, 19 (2020) 585–592.
62. H. Li, R. Chen, M. Ali, H. Lee, M.J. Ko, *Adv. Funct. Mater.* (2020) 2002739.
63. M. Hu, C. Cui, C. Shi, Z.-S. Wu, J. Yang, R. Cheng, T. Guang, H. Wang, H. Lu, X. Wang, *ACS Nano*, 13 (2019) 6899–6905.
64. S. Nam, S. Umrao, S. Oh, K.H. Shin, H.S. Park, I.-K. Oh, *Compos. Part B Eng.*, 181 (2020) 107583.
65. C. Sun, X. Shi, Y. Zhang, J. Liang, J. Qu, C. Lai, *ACS Nano*, 14 (2020) 1176–1184.
66. J. Luo, C. Fang, C. Jin, H. Yuan, O. Sheng, R. Fang, W. Zhang, H. Huang, Y. Gan, Y. Xia, C. Liang, J. Zhang, W. Li, X. Tao, *J. Mater. Chem. A*, 6 (2018) 7794–7806.
67. S. Sun, C. Liao, A.M. Hafez, H. Zhu, S. Wu, *Chem. Eng. J.*, 338 (2018) 27–45.
68. H. Zhou, Y. Lu, F. Wu, L. Fang, H. Luo, Y. Zhang, M. Zhou, *J. Alloys Compd.*, 802 (2019) 259–268.
69. W. Liu, Z. Wang, Y. Su, Q. Li, Z. Zhao, F. Geng, *Adv. Energy Mater.*, 7 (2017) 1602834.
70. C. (John) Zhang, L. Cui, S. Abdolhosseinzadeh, J. Heier, *InfoMat*, 2 (2020) 613–638.
71. X. Wang, S. Lin, H. Tong, Y. Huang, P. Tong, B. Zhao, J. Dai, C. Liang, H. Wang, X. Zhu, Y. Sun, S. Dou, *Electrochimica Acta*, 307 (2019) 414–421.
72. S. Zhang, H. Ying, R. Guo, W. Yang, W.-Q. Han, *J. Phys. Chem. Lett.*, 10 (2019) 6446–6454.
73. Z. Ling, C.E. Ren, M.-Q. Zhao, J. Yang, J.M. Giammarco, J. Qiu, M.W. Barsoum, Y. Gogotsi, *Proc. Natl. Acad. Sci.*, 111 (2014) 16676–16681.
74. P. Sobolčiak, A. Ali, M.K. Hassan, M.I. Helal, A. Tanvir, A. Popelka, M.A. Al-Maadeed, I. Krupa, K.A. Mahmoud, *PLoS One*, 12 (2017) e0183705.
75. F. Wang, C. Yang, C. Duan, D. Xiao, Y. Tang, J. Zhu, *J. Electrochem. Soc.*, 162 (2014) B16.
76. T. Li, L. Chen, X. Yang, X. Chen, Z. Zhang, T. Zhao, X. Li, J. Zhang, *J. Mater. Chem. C*, 7 (2019) 1022–1027.

77. Y. Guo, M. Zhong, Z. Fang, P. Wan, G. Yu, *Nano Lett.*, 19 (2019) 1143–1150.
78. Y. Gao, C. Yan, H. Huang, T. Yang, G. Tian, D. Xiong, N. Chen, X. Chu, S. Zhong, W. Deng, *Adv. Funct. Mater.*, 30 (2020) 1909603.
79. Y. Yue, N. Liu, W. Liu, M. Li, Y. Ma, C. Luo, S. Wang, J. Rao, X. Hu, J. Su, Z. Zhang, Q. Huang, Y. Gao, *Nano Energy*, 50 (2018) 79–87.
80. X.-Y. Yang, W. Luo, R. Ahuja, *Nano Energy* (2020) 104911.